Journal of Thermal Analysis and Calorimetry (2023) 148:13233–13243
https://doi.org/10.1007/s10973-023-12623-1

Silver/polydopamine/HMX nanocomposite: novel functionalized catalyzed energetic matrix with superior decomposition kinetics

Sherif Elbasuney[1,2] · Shukri Ismael[2] · M. Yehia[2] · Ahmed Saleh[3]

Received: 14 August 2022 / Accepted: 25 September 2023 / Published online: 25 October 2023

Abstract

Surface engineering of energetic materials can secure novel decomposition characteristics. Nature can inspire novel solutions. Polydopamine, with strong adhesion power of mussel proteins, can open new venues for the facile development of functionalized energetic materials. HMX, one of the most powerful energetic materials in use, was surface modified with PDA. The reactive amine groups of PDA surfactant were employed for noble metal catalyst deposition. Silver nanocatalyst was deposited on HMX surface. Uniform deposition of silver nanocatalyst was assessed using EDAX detector. Decomposition kinetics was investigated via isoconversional (model free) and model fitting. Kissinger, Kissinger–Akahira–Sunose (KAS), integral isoconversional method of Ozawa, Flynn, and Wall (FWO), and differential isoconversional method of Friedman. Silver nanocatalyst offered an increase in HMX decomposition enthalpy by 32.4%. In the meantime, HMX activation energy was decreased from 350 ± 2.53 to 284.9 ± 1.5 kJ mol^{-1} by Friedman method. Silver nanocatalyst could combust exothermically; it could induce condensed phase reactions that could boost HMX decomposition. Silver nanocatalyst experienced change in HMX decomposition model from diffusion reaction (D_1) to (A_3) known as three-dimensional random nucleation and growth. Surface modification with PDA secured enhanced HMX sensitivity to falling mass impact by 40%.

Keywords Surface modification · Catalyst · Energetic materials · Nanocomposite

Introduction

Energetic materials are coated with inert polymers, in an attempt to improve the sensitivity and to reduce hazardous risks. In the meantime, inert polymers could decrease energetic material performance [1]. Balanced performance and sensitivity of energetic material is mandatory for advanced energetic systems [2]. High performance can be accomplished via integration of reactive metal particles; however, sensitivity stays a major challenge [3]. Surface modification with novel polymeric surfactant can offer narrative solutions; however, inert polymers could negatively impact energetic material performance. Mussel proteins with strong adhesive power inspire researchers for surface modification with catecholic (1, 2-dihydroxybenzene), known as dopamine [4–6]. Dopamine can undergo auto-polymerization in aerated buffered solution to develop polydopamine (PDA) [7–9]. PDA can offer durable polymeric layer of 50-nm thickness at the substrate surface [10]. Additionally, PDA can secure strong binding to hydrophilic and hydrophobic surfaces via hydrogen or coordination bonding, respectively [11].

PDA can bind strongly to HMX via hydrogen bonding with nitro group. Furthermore, PDA can induce coordination with CH_2 groups of HMX heterocyclic ring [12]. Therefore, durable polymeric surfactant layer could be developed [10]. PDA surfactant with reactive amine and hydroxyl functional groups can offer novel characteristics. PDA can induce secondary chemical reactions; PDA surfactant has unique reducing ability to deposit noble metal particles (Fig. 1) [13, 14].

These characteristics could diversify the reactivity and functionality of energetic materials [15]. The surface of energetic material can be functionalized with novel catalyst particles. Noble metal particles, with partially filled d-shell electrons, can experience novel catalytic properties. They could induce different secondary reactions in the condensed

✉ Sherif Elbasuney
sherif_basuney2000@yahoo.com; s.elbasuney@mtc.edu.eg

[1] Nanotechnology Research Centre, Military Technical College, Cairo, Egypt

[2] School of Chemical Engineering, Military Technical College, Cairo, Egypt

[3] Science and Technology Center of Excellence, Cairo, Egypt

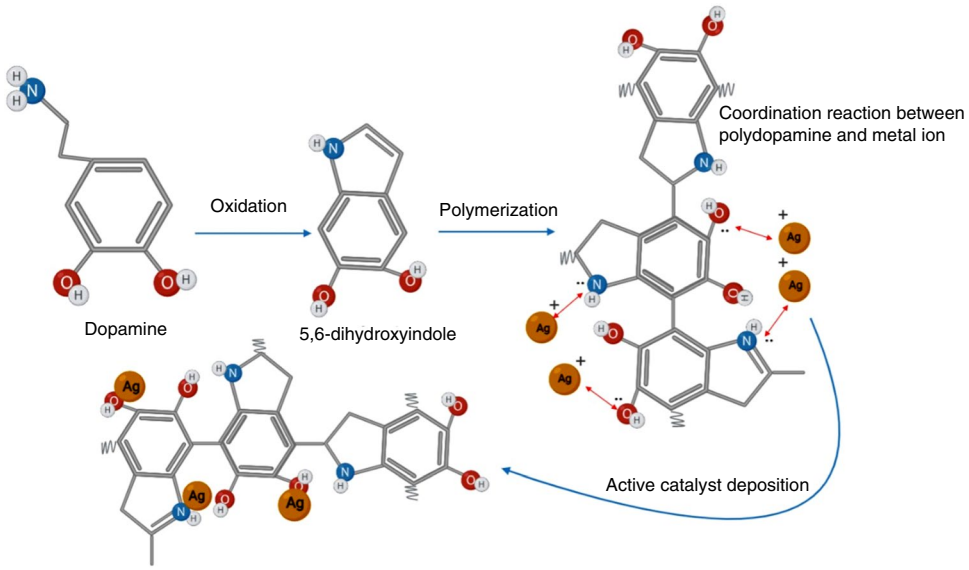

Fig. 1 Mechanism of auto-polymerization of dopamine and reactive metal deposition

phase, with decrease in the required activation energy [16]. Furthermore, noble metal particles could be oxidized exothermically to metal oxide; the evolved oxide could act as a reactive surface for secondary reactions. Noble metal catalyst can not only reduce the required activation energy; but also it could boost decomposition enthalpy [17]. Silver is one of the most common catalyst particles for energetic systems [18]. Silver is the universal oxidizer for decomposition of hydrogen peroxide [19, 20]. Silver can offer novel decomposition kinetics toward wide range of energetic materials [21, 22]. HMX is one of the most powerful energetic materials; modification with PDA can offer adhesive durable surfactant layer of 50-nm thickness [4, 23]. PDA can enhance HMX sensitivity; in the meantime, PDA surfactant can be employed to deposit silver nanocatalyst on HMX surface. This approach can offer direct contact between the catalyst particles and the energetic material [24, 25]. Recently, much attention has been directed to the deposition of reactive catalyst particles that could offer novel decomposition kinetic parameters [26, 27].

In this study, HMX energetic matrix was surface modified with PDA via auto-polymerization at the particle surface. The flexible reactivity of PDA surfactant was exploited to deposit silver nanocatalyst on HMX surface. Uniform dispersion of silver nanocatalyst on HMX was assessed via EDAX analysis. The impact of silver nanocatalyst on HMX thermal behaviour was evaluated using DSC and TGA. Ag/PDA/HMX demonstrated novel thermal behaviour with an increase in decomposition enthalpy by 32.4%. Silver nanocatalyst demonstrated decrease in HMX activation energy from 350 ± 2.53 to 284.9 ± 1.5 kJ mol^{-1} by Friedman method. This means that high propagation reaction can be achieved. In the meantime, surface modification with PDA offered increase in HMX sensitivity to impact by 45% (Table 1).

Experimental

Development of Ag/PDA/HMX nanocomposite

Surface modification with PDA offers facile technology that can avoid violent conditions [28]. Starting HMX particles was disseminated in deionized water via ultrasonic probe homogenizer. Colloidal HMX particles were oxygenated for 1 h by bubbling oxygen gas. Dopamine hydrochloride (Aldrich, 99%) was dissolved in HMX slurry and buffered to pH 9. Auto-polymerization of dopamine was conducted in batch reactor for 4 h with continuous stirring. Surface modified HMX was filtered and washed with deionized water. PDA/HMX particles were dispersed in silver nitrate solution under vigorous stirring using batch reactor for deposition of silver nanocatalyst on the surface of PDA/HMX.

Table 1 Kinetic parameters for virgin HMX and Ag/PDA/HMX nanocomposite

Samples	Methods	E_a/KJ mol^{-1}	Log/A s^{-1}
HMX	FWO	342.3 ± 10.5	31.2 ± 1.07
	KAS	345.4 ± 12	33.4 ± 1.12
	Friedman	350 ± 2.53	25.3 ± 0.89
	Kissinger	360.6 ± 0.3	27.8 ± 0.32
Ag/PDA/HMX	FWO	290.1 ± 1.21	20.2 ± 1.73
	KAS	294.5 ± 3.2	18.8 ± 1.72
	Friedman	284.9 ± 1.5	23 ± 3.2
	Kissinger	302 ± 0.54	21.05 ± 1.33

Characterization of Ag/PDA/HMX nanocomposite

Morphology of starting HMX and Ag/PDA/HMX was visualized with SEM (ZEISS SEM EVO); dispersion of deposited silver nanocatalyst was investigated using EDAX detector. Crystalline structure of HMX and Ag/PDA/HMX nanocomposite was investigated using Hilton-brooks X-ray diffractometer. Chemical structure of HMX and Ag/PDA/HMX was further investigated using FTIR spectrometer (Shimazu 8400).

Thermal behaviour of Ag/PDA/HMX nanocomposite

Thermal behaviour of Ag/PDA/HMX nanocomposite was investigated to virgin HMX. Decomposition enthalpy of Ag/PDA/HMX nanocomposite was evaluated using DSC Q20 by TA. Mass loss with temperature of Ag/PDA/HMX nanocomposite was investigated using TGA 55 by TA. Tested sample was heated from 50 to 500 °C, at 10 °C min^{-1}.

Decomposition kinetics of Ag/PDA/HMX

The decomposition kinetic of Ag/PDA/HMX was evaluated using different analysis models including isoconversional (model free) and model fitting. Kissinger, Kissinger–Akahira–Sunose (KAS), differential isoconversional method of Friedman, and integral isoconversional method of Ozawa, Flynn, and Wall (FWO) models were adopted for decomposition kinetic study [29, 30]. Decomposition kinetic of HMX and Ag/PDA/HMX composite was assessed using TGA. The mass loss of tested sample was recorded at different heating rates 4, 6, 8, and 10 °C min^{-1}.

The equations for the FWO and KAS methods are given below.

$$\text{FWO:}\quad \ln\beta_{\mathrm{i}} = \ln\left(\frac{A\alpha E_{\alpha}}{Rg(\alpha)}\right) - 5.331 - 1.052\frac{E_{\alpha}}{RT\alpha,i} \tag{1}$$

$$\text{KAS}:\quad \ln\left(\frac{\beta_{\mathrm{i}}}{T^{1.92}_{\alpha,\mathrm{i}}}\right) = \text{Const} - 1.0008\frac{E\alpha}{RT\alpha} \tag{2}$$

$$\text{Friedman}:\quad \ln\left[\beta_{\mathrm{i}}\left(\frac{\mathrm{d}\alpha}{\mathrm{d}T}\right)_{T_{\alpha,\mathrm{i}}}\right] = \ln\left(A_{\alpha}f(\alpha)\right) - \frac{E\alpha}{RT_{\alpha,\mathrm{i}}} \tag{3}$$

For precise calculations, a new modified Friedman isoconversional method was proposed [31]

$$\left(\frac{\mathrm{d}\alpha}{\mathrm{d}T}\right)_{T_{\alpha,\mathrm{i}}} \approx \left(\frac{\Delta\alpha}{\Delta T}\right)_{T_{\alpha,\mathrm{i}}} = \frac{\Delta\alpha}{T_{\alpha+\Delta\alpha/2,i} - T_{\alpha-\Delta\alpha/2,\mathrm{i}}} \tag{4}$$

With the substitution of Eq. 4 into Eq. 3, the modified Friedman (Eq. 5) was obtained.

$$\text{Modified Friedman:}\quad \ln\left[\beta_{\mathrm{i}}\frac{\Delta\alpha}{T_{\alpha+\frac{\Delta\alpha}{2},\mathrm{i}} - T_{\alpha-\frac{\Delta\alpha}{2},\mathrm{i}}}\right] = \ln\left(A_{\alpha}f(\alpha)\right) - \frac{E\alpha}{RT_{\alpha,\mathrm{i}}} \tag{5}$$

To get the kinetic parameters (E_{a}, A), a linear equation was obtained by drawing $\ln\beta_{\mathrm{i}}$ versus $1000/T_{\alpha,\mathrm{i}}$, $\ln\left(\frac{\beta_{\mathrm{i}}}{T^{1.92}_{\alpha,\mathrm{i}}}\right)$ versus $1000/T_{\alpha,\mathrm{i}}$, and $\ln\left[\beta_{\mathrm{i}}\frac{\Delta\alpha}{T_{\alpha+\frac{\Delta\alpha}{2},i} - T_{\alpha-\frac{\Delta\alpha}{2},\mathrm{i}}}\right]$ versus $1000/T_{\alpha,\mathrm{i}}$. The slope was the effective activation energy (E_{a}); the intercept was the frequency factor (A). The subscript i represented the ith heating rate; the subscript α was the value related to the conversion degree; β was the heating rate; and T was the decomposition temperature. Activation energy (E_{a}) of developed Ag/PDA/HMX was evaluated from Kissinger model (Eq. 6) [32, 33],

$$-\frac{E_{\mathrm{a}}}{R} = \frac{\mathrm{d}\ln(\beta/T_{\mathrm{p}}^2)}{\mathrm{d}(1/T_{\mathrm{p}})} \tag{6}$$

where β was the heating rate, T_{p} was the decomposition temperature, and R was the universal gas constant.

Results and discussion

Characterization of Ag/PDA/HMX

Starting HMX demonstrated irregular particles of 200-µm size. Ag/PDA/HMX nanocomposite experienced uniform deposition of silver nanocatalyst on HMX surface as white points (Fig. 2).

Elemental mapping using EDAX detector demonstrated uniform dispersion of silver nanocatalyst on HMX surface (Fig. 3). This fabrication technology not only offered uniform catalyst dispersion; but also direct contact between the catalyst particles and the energetic material surface.

Quantification of deposited silver was evaluated using EDAX detector; silver content of 1.35 mass% was reported from EDAX analysis (Fig. 4).

This novel catalyst deposition approach can offer novel catalytic activity due to the direct contact between catalyst particles and energetic matrix [34]. Chemical strucutre of Ag/PDA/HMX nanocomposite and HMX was investigated using FTIR spectrocopy. Chemical strucutre of Ag/PDA/HMX nanocomposite was investigated using FTIR spectrocopy. Ag/PDA/HMX nancomposite demonstrated fingerprint region (910–1300 cm^{-1}) similar to virgin HMX. Virgin HMX demonstrated ring bending and streching at

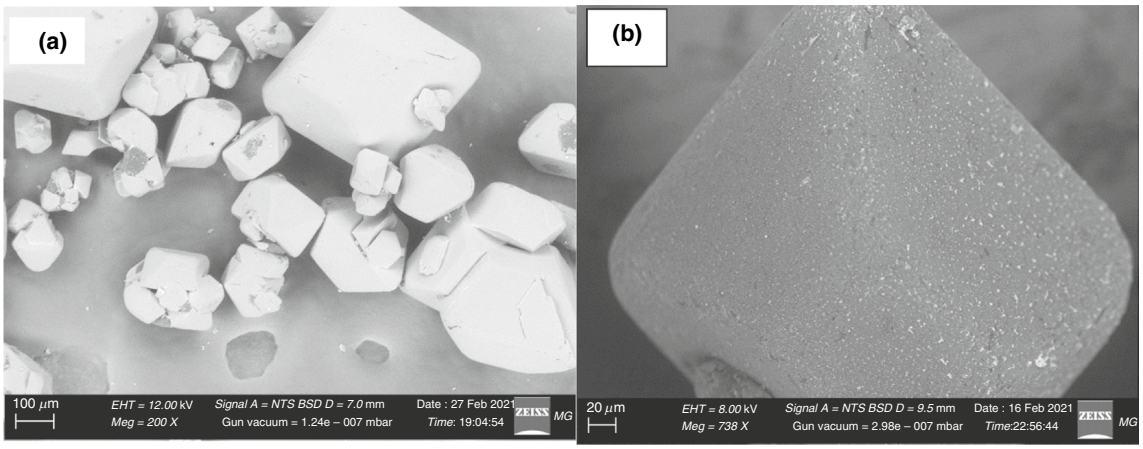

Fig. 2 SEM micrographs of starting HMX (**a**) and Ag/PDA/HMX nanocomposite (**b**)

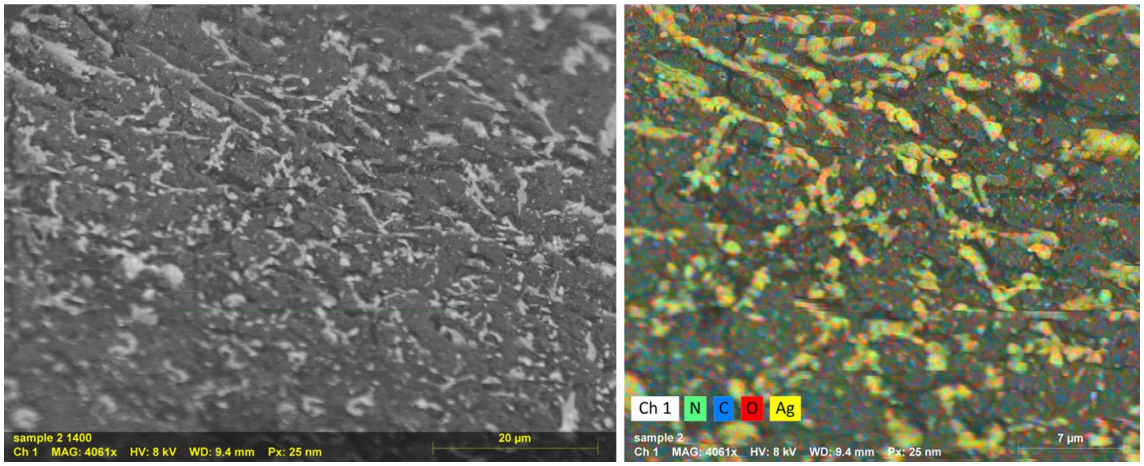

Fig. 3 Dispersion of Ag nanocatalyst on the surface of HMX

942.06 and 961.82 cm^{-1}, CH_2 bending at 1332.57 cm^{-1}, NO_2 bending out of plane at 761.74 cm^{-1}, and NO_2 asymmetric stretching 1552.9 cm^{-1}. This confirmed similar chemical structure. The variation between Ag/PDA/HMX nanocomposite to virgin HMX was observed over function group region (4000–1300 cm^{-1}). Ag/PDA/HMX nanocomposite experienced intense absorption in function group region; this could be ascribed to surface modification with PDA. Ag/PDA/HMX peaks were correlated to O–H and N–H stretch of PDA surfactant over the band 3200–3500 cm^{-1} (Fig. 5).

The crystalline structure of Ag/PDA/HMX demonstrated high crystalline structure similar to virgin HMX. The main characteristic peaks at 2Θ values of 38.117 and 44.279 were correlated to deposited silver planes at (1,1,1) and (2,0,0), respectively, related (Fig. 6). The low counts of silver characteristic peaks could be correlated to its limited amount (1.35 mass%).

Thermal behaviour of Ag/PDA/HMX nanocomposite

Decomposition enthalpy of Ag/PDA/HMX nanocomposite was investigated to virgin HMX using DSC. Whereas Ag/PDA/HMX nanocomposite demonstrated decomposition enthalpy of 1354 J g^{-1}; virgin HMX demonstrated decomposition enthalpy of 1016 J g^{-1} (Fig. 7).

The surge increase in HMX decomposition enthalpy could be ascribed to the induced condensed phase reactions due to silver catalyst. Silver can induce complex reactions within the condensed phase due to partially filled d-shell orbital [35]. Decomposition gaseous products could be adsorbed on the catalyst surface. These features could boost HMX decomposition enthalpy. Ag/PDA/HMX nanocomposite demonstrated decrease in HMX main decomposition temperature by 5 °C. Thermal behaviour of Ag/PDA/HMX nanocomposite was assessed using TGA (Fig. 8).

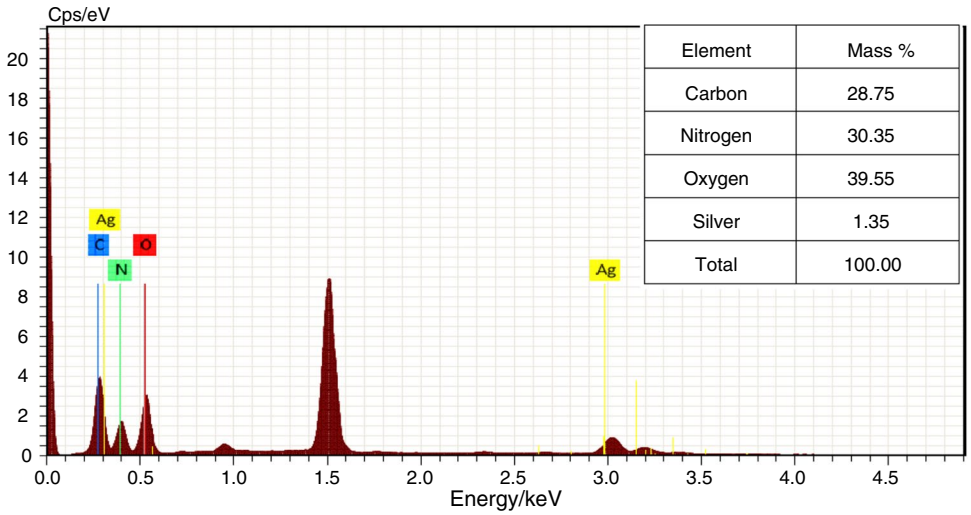

Fig. 4 Elemental composition of Ni/PDA/HMX nanocomposite

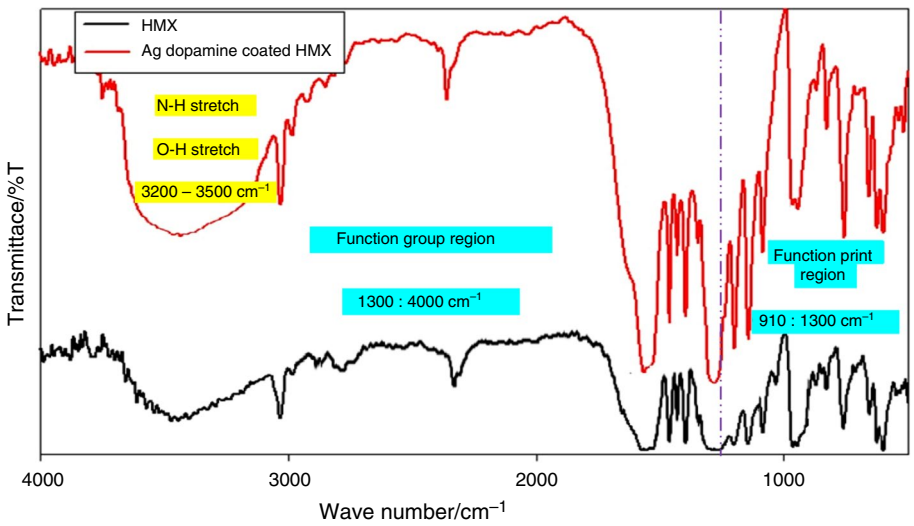

Fig. 5 FTIR spectra of Ag/PDA/HMX to virgin HMX

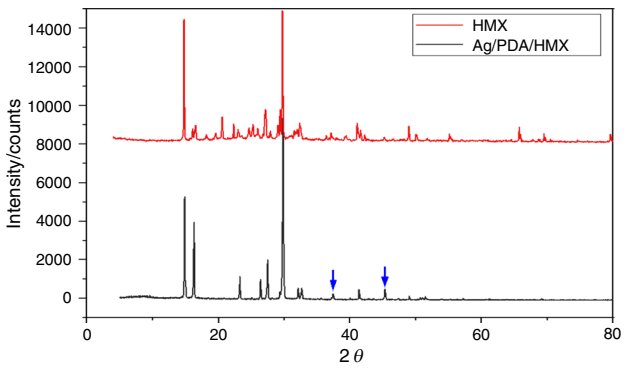

Fig. 6 XRD diffractogram of Ag/PDA/HMX nanocomposite to virgin HMX

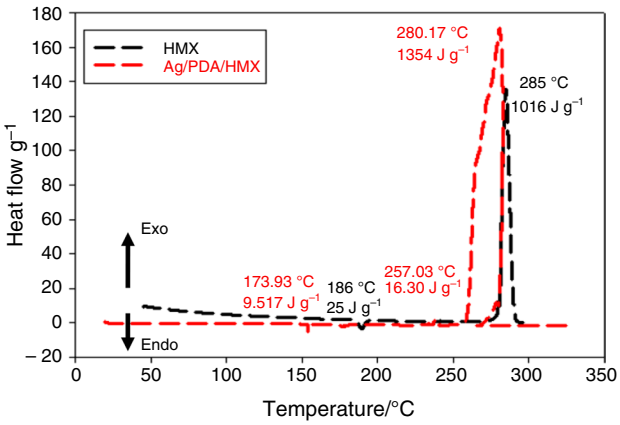

Fig. 7 Thermal behaviour of Ag/PDA/HMX nanocomposite to pure HMX using DSC

TGA outcomes were found to be in good accordance with DSC results; the catalytic effect of silver nanocatalyst could withstand the decrease in HMX main decomposition temperature. Dopamine has a reducing capability to many metals such as Pd, Ag, and Au [36–38]. PDA surfactant secured a high homogeneity and direct contact between the silver nanocatalyst and HMX surface. Silver nanoparticles could react as a fuel with oxidizing fragments evolved from HMX; with the exclusive formation of silver oxides nanoparticles. Silver oxides could react as a catalyst to decrease the decomposition temperature and activation energy of HMX (Fig. 9).

Sensitivity to impact of Ag/PDAHMX nanocomposite was evaluated to virgin HMX by falling hammer method. Whereas HMX demonstrated initiating impulse of 7.40 Nm; Ag/PDA/HMX nanocomposite demonstrated 10.36 Nm. It can be concluded that PDA surfactant not only secured nanocatalyst deposition; but also enhanced sensitivity to impact.

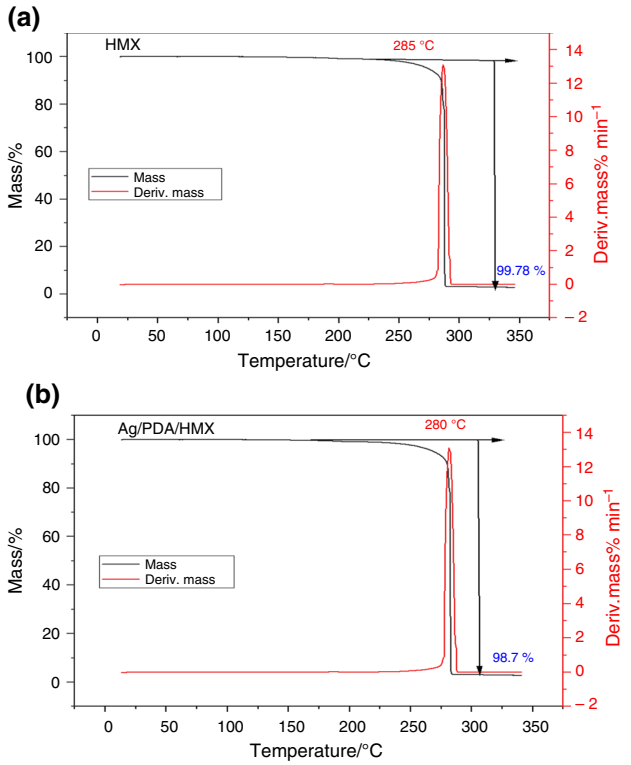

Fig. 8 Thermal behaviour of Ag/PDA/HMX nanocomposite to pure HMX using TGA

Kinetic analysis

TGA analysis at different heating rates was adopted to examine the thermocatalytic decomposition mechanism of Ag/PDA/HMX (Fig. 10) [29, 30].

According to the sets of α (the conversion rate)-T plots (Fig. 11); a series of kinetic triplets can be obtained via the isoconversional pathways (FWO, KAS, and Friedman equations).

The $\ln \beta_i$ versus $1000/T_{\alpha,i}$, $\ln\left(\frac{\beta_i}{T_{\alpha,i}^{1.92}}\right)$ versus $1000/T_{\alpha,i}$, and $\ln\left[\beta_i \frac{\Delta\alpha}{T_{\alpha+\frac{\Delta\alpha}{2},i} - T_{\alpha-\frac{\Delta\alpha}{2},i}}\right]$ versus $1000/T_{\alpha,I}$ curves corresponding to FWO, KAS, and Friedman models over the range of $\alpha = 0.05 \sim 0.9$, with a step size of 0.05, are demonstrated in Fig. 12.

Virgin HMX demonstrated similar E_a value using Friedman, FWO, and KAS models, respectively. Virgin HMX demonstrated dramatic increase in E_a with increase in conversion extent (α). Activation energy for Ag/PDA/HMX nanocomposite obtained from FWO, and KAS methods demonstrated slight changes with α. Ag/PDA/HMX nanocomposite demonstrated similar behaviour using KAS and FWO models; E_a value was almost constant with conversion extent α. In the meantime, Friedman model demonstrated an increase in E_a value with α increase up to = 0.55; subsequently, E_a value was decreased with increase in α to = 0.95 (Fig. 13).

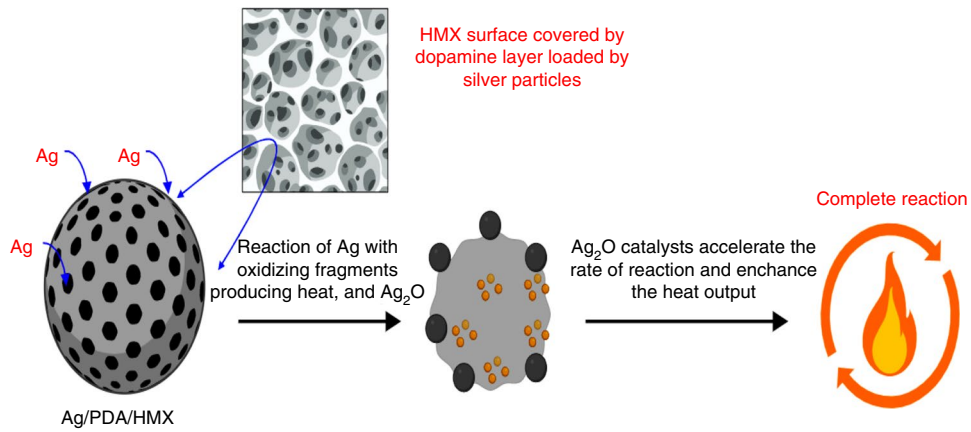

Fig. 9 Schematic of the thermal decomposition mechanism of Ag/PDA/HMX nanocomposite

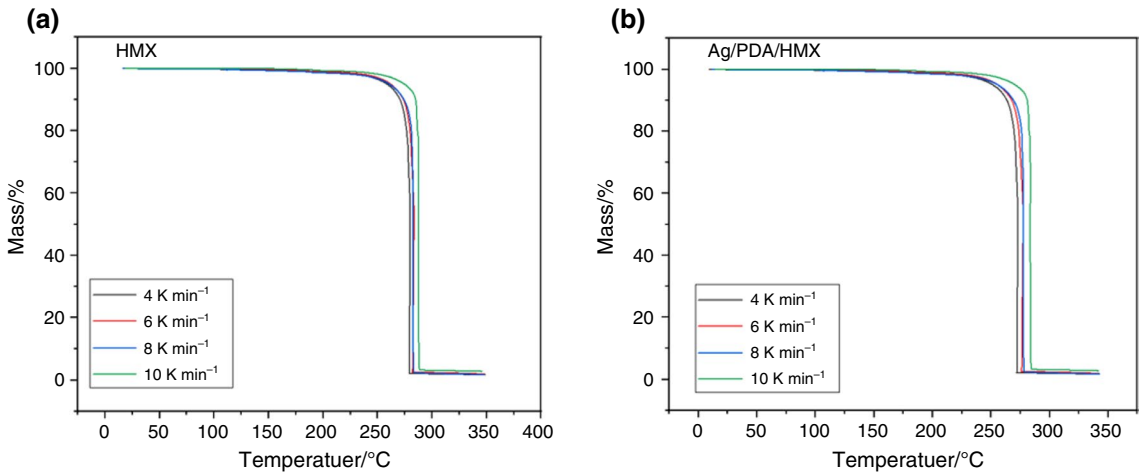

Fig. 10 TGA curves of virgin HMX (**a**) and Ag/PDA/HMX nanocomposite (**b**) at different heating rates

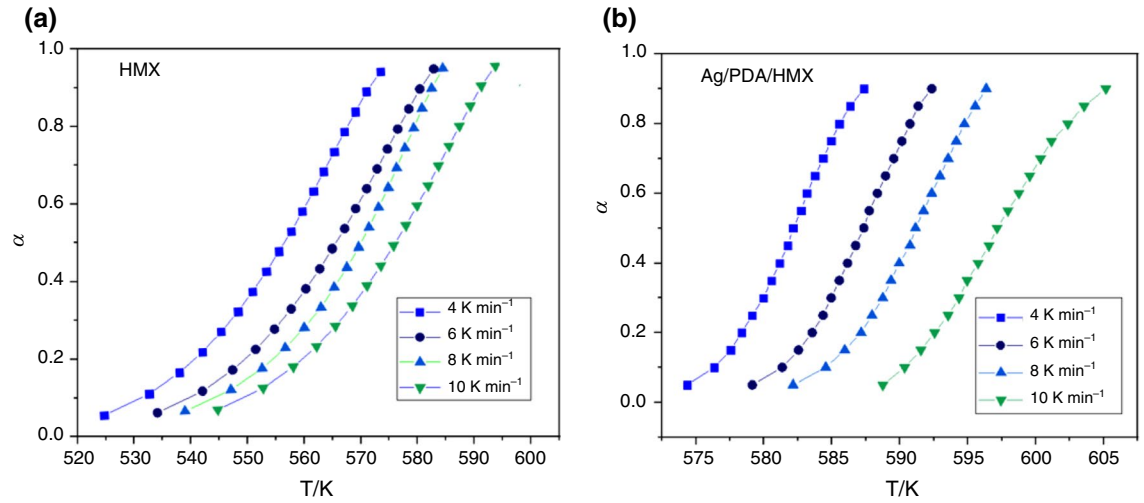

Fig. 11 α-T curves of virgin HMX (**a**) and Ag/PDA/HMX nanocomposite (**b**) at different heating rates

E_α value of Ag/PDA/HMX nanocomposite by the Friedman was found to be 284.9 kJ mol^{-1} compared with 350.1 kJ mol^{-1} for virgin HMX. Ag/PDA/HMX nanocomposite demonstrated low activation energy compared to virgin HMX; this revealed the potential catalytic activity of silver on HMX decomposition. E_a was evaluated for virgin HMX and Ag/PDA/HMX nanocomposite via Kissinger model. Activation energy was retrieved from the slop of the straight line of $\ln(\beta/T^2)$ versus $(1/T)$ (Fig. 14).

Silver nanocatalyst experienced decrease in HMX activation energy by 16.1%. The activation energy of virgin HMX and Ag/PDA/HMX nanocomposite was reported to be 360.6 and 302.5 kJ mol^{-1}, respectively. Silver catalytic performance could be ascribed to the strong bonding of deposited nanocatalyst on the energetic material surface.

The main pyrolysis mechanisms and the corresponding model relationships are demonstrated in Supplementary Table T1 [39]. The final pyrolysis reaction model was determined by Coats–Redfern (CR) method. The corresponding model functions (Supplementary Table T1) were introduced in Eq. (4). $\ln\left(\frac{g(\alpha)}{T^2}\right) - 1/T$ curves for each tested sample were plotted by CR method (Fig. 15).

The kinetic decomposition model for pure HMX and Ag/PDA/HMX nanocomposite was investigated via CR method. The kinetic model for virgin HMX decomposition was a diffusion reaction (D_1), while the model for Ag/PDA/HMX nanocomposite was changed to (A_3) known as a random nucleation followed by three-dimensional random nucleation and nucleation growth. It was verified that the Ag/PDA has a catalytic effect on HMX decomposition by decreasing the

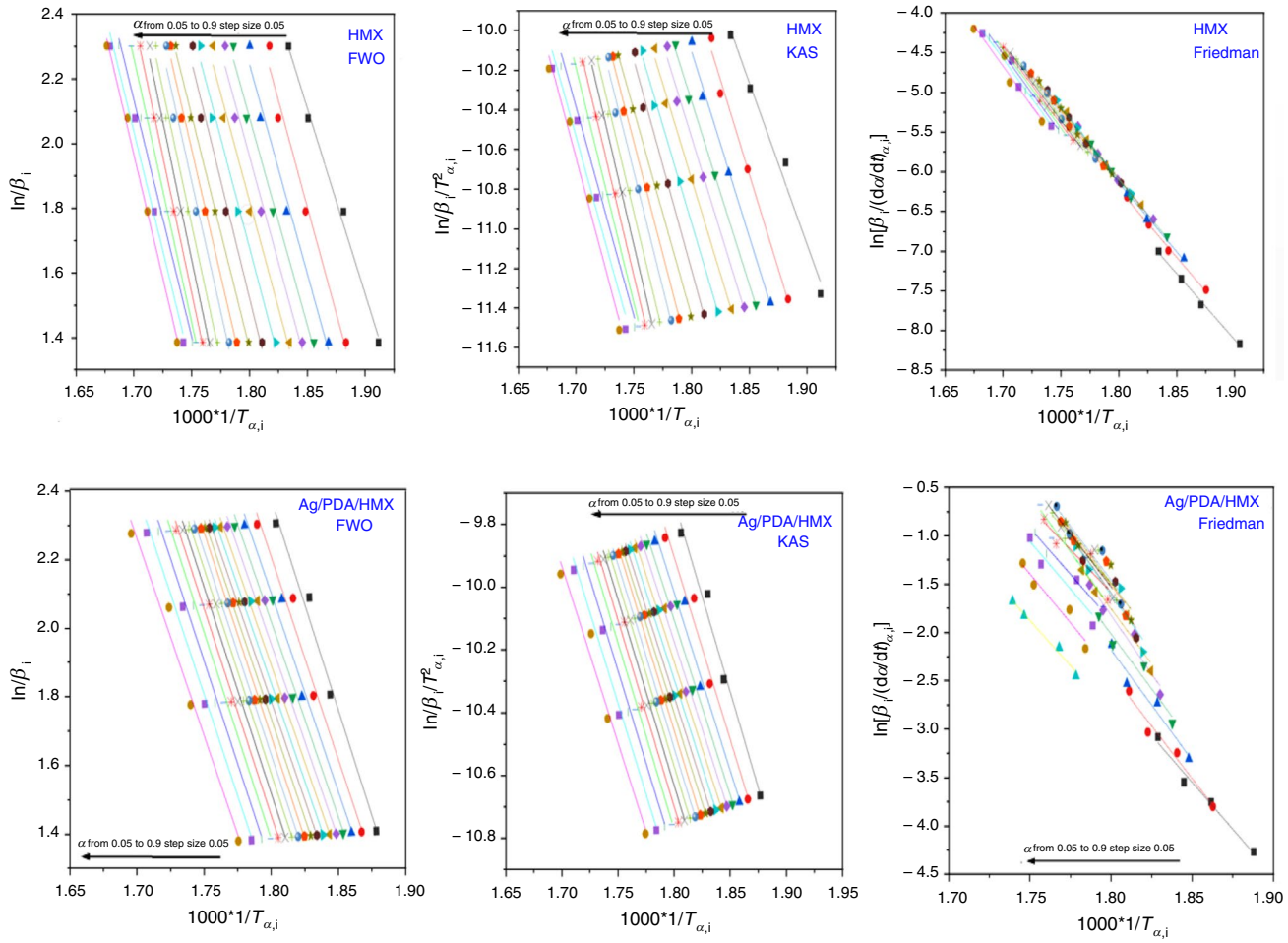

Fig. 12 Global kinetic profiles of virign HMX and Ag/PDA/HMX nanocomposite

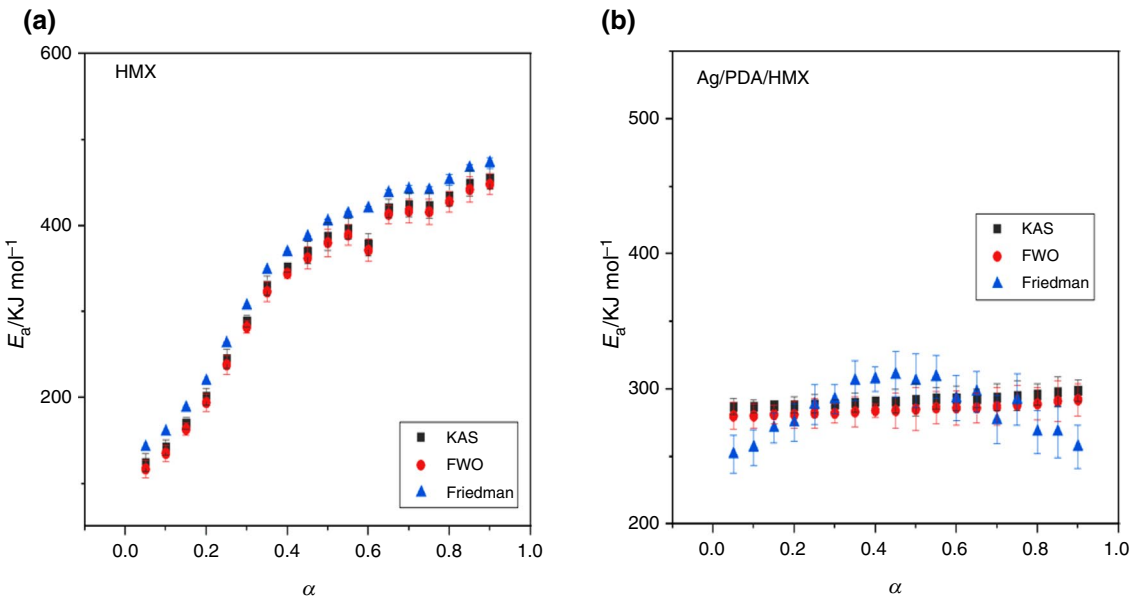

Fig. 13 E_a versus α curves of HMX (**a**) and Ag/PDA/HMX nanocomposite (**b**)

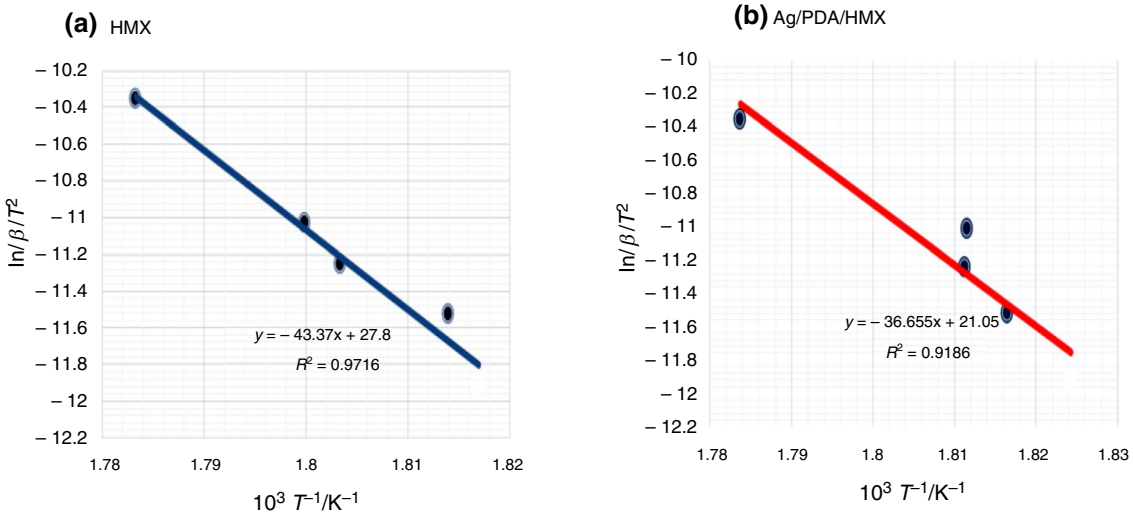

Fig. 14 Activation energy of Ag/PDA/HMX to virign HMX

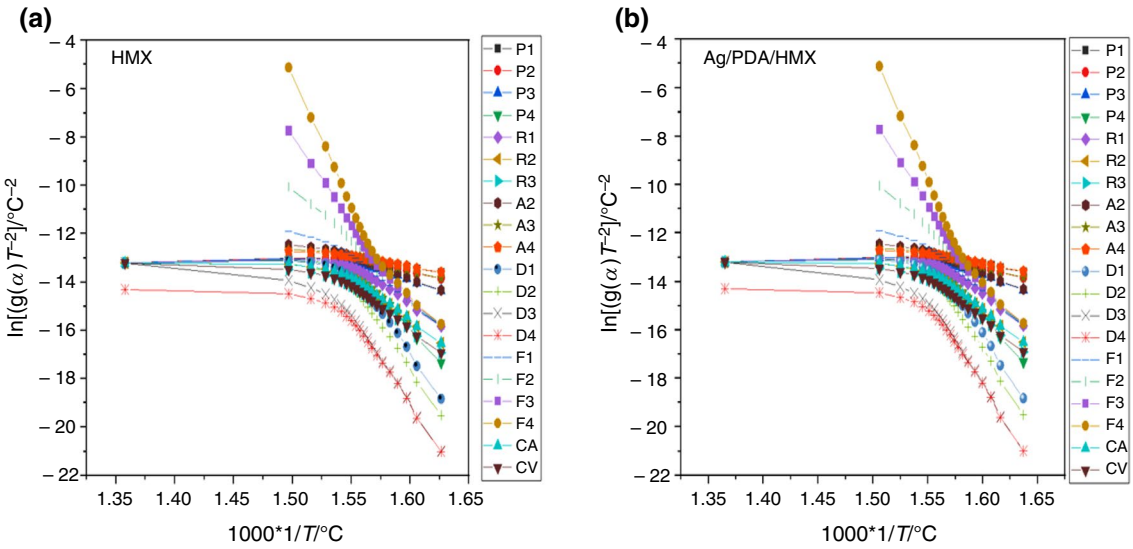

Fig. 15 The reaction mechanisms of the two samples at each stage using CR method

decomposition temperature, increase the heat evolved, and change the mechanism of reaction from (D_1) to (A_3) model.

Conclusion and future work

Facile surface modification with dopamine was adopted for surface modification of HMX energetic matrix. Dopamine auto-polymerization at the solid surface was conducted. The reactivity of amine groups of PDA polymeric surfactant was employed to deposit silver nanocatalyst on HMX surface. Uniform deposition of silver nanocatalyst on HMX surface was verified using EDAX detector. Silver nanocatalyst experienced an increase in HMX decomposition enthalpy by 32.4% using DSC. Silver nanocatalyst offered decrease in HMX activation energy was decreased from 350.1 to 284.9 kJ mol^{-1} by Friedman model. Additionally, silver nanocatalyst demonstrated change in HMX decomposition model from diffusion reaction (D1) to (A3) known as a random nucleation followed by three-dimensional random nucleation and nucleation growth. Furthermore, PDA surfactant offered enhanced sensitivity to impact by 40%.

Supplementary Information The online version contains supplementary material available at https://doi.org/10.1007/s10973-023-12623-1.

Acknowledgements The authors would like to thank Chemical Engineering Department, Military Technical College (MTC), Egyptian Armed Forces, Cairo, Egypt, and ZEISS microscope team at Cairo,

Egypt, for their invaluable support of this study. Figures 1, 2, 4, and 11 were created by Bio Render programme.

Funding Open access funding provided by The Science, Technology & Innovation Funding Authority (STDF) in cooperation with The Egyptian Knowledge Bank (EKB).

Declarations

Conflict of interest The authors declare that they have no conflict of interest.

References

1. Parker GR, et al. Direct observation of frictional ignition in dropped HMX-based polymer-bonded explosives. Combust Flame. 2020;221:180–93.
2. Anderson EK, Chiquete C, Jackson SI. Experimental measurement of energy release from an initiating layer in an insensitive explosive. Proc Combust Inst. 2021;38(3):3733–40.
3. Zhao G, et al. One-step synthesis to an insensitive explosive: N, N′-bis((1H-tetrazol-5-yl)methyl)nitramide (BTMNA). Chem Eng J. 2021;412:128697.
4. He W, et al. Mussel-inspired polydopamine-directed crystal growth of core-shell n-Al@PDA@CuO metastable intermixed composites. Chem Eng J. 2019;369:1093–101.
5. You I, et al. Enhancement of blood compatibility of poly (urethane) substrates by mussel-inspired adhesive heparin coating. Bioconjug Chem. 2011;22(7):1264–9.
6. Zhang X, et al. Mussel-inspired fabrication of functional materials and their environmental applications: progress and prospects. Appl Mater Today. 2017;7:222–38.
7. Jiang J, et al. Surface characteristics of a self-polymerized dopamine coating deposited on hydrophobic polymer films. Langmuir. 2011;27(23):14180–7.
8. Molitor P, Barron V, Young T. Surface treatment of titanium for adhesive bonding to polymer composites: a review. Int J Adhes Adhes. 2001;21(2):129–36.
9. Fang Y, et al. Polydopamine nanotube for dual bio-inspired strong, tough, and flame retarding composites. Compos B Eng. 2020;197:108184.
10. Elbasuney S, Yehia M, El-Sayyad GS. Bio-inspired metastable intermolecular nanothermite composite based on Manganese dioxide/Polydopamine/Aluminium. J Mater Sci Mater Electron. 2021;32(7):9158–70.
11. El Yakhlifi S, Ball V. Polydopamine as a stable and functional nanomaterial. Colloids Surf B. 2020;186:110719.
12. Xu Z, Miyazaki K, Hori T. Fabrication of polydopamine-coated superhydrophobic fabrics for oil/water separation and self-cleaning. Appl Surf Sci. 2016;370:243–51.
13. Bock N, et al. Polydopamine coating of uncrosslinked chitosan as an acellular scaffold for full thickness skin grafts. Carbohydr Polym. 2020;245:116524.
14. Lin C, et al. Controllable tuning of energetic crystals by bioinspired polydopamine. Energ Mater Front. 2020;1(2):59–66.
15. Elbasuney S. Novel colloidal nanothermite particles (MnO_2/Al) for advanced highly energetic systems. J Inorg Organomet Polym Mater. 2018;28(5):1793–800.
16. Zarko VE, Gromov AA, editors. Energetic nanomaterials synthesis, characterization, and application. Amsterdam: Elsevier; 2016.
17. Spitzer D, et al. Energetic nano-materials: opportunities for enhanced performances. J Phys Chem Solids. 2010;71(2):100–8.
18. Galwey AK, Mohamed MA, Cromie DS. Role of silver compounds in promoting the thermal decomposition of ammonium perchlorate. React Solids. 1986;1(3):235–51.
19. Chan Y-A, Hsu H-W, Chao Y-C. Development of a HTP monopropellant thruster by using composite silver catalyst. In: 47th AIAA/ASME/SAE/ASEE joint propulsion conference & exhibit. 2011.
20. Lee S-L, Lee C-W. Performance characteristics of silver catalyst bed for hydrogen peroxide. Aerosp Sci Technol. 2009;13(1):12–7.
21. Amri R, Gibbon D, Rezoug T. The design, development and test of one newton hydrogen peroxide monopropellant thruster. Aerosp Sci Technol. 2013;25(1):266–72.
22. Reid S, et al. Towards an advanced 3D-printed catalyst for hydrogen peroxide decomposition: development and characterisation. Catal Today. 2023;418:114155.
23. Elbasuney S, Ismael S, Yehia M. Ammonium percholorate/HMX co-crystal: bespoke energetic materials with tailored decomposition kinetics via dual catalytic effect. J Energ Mater. 2023;41(3):429–48.
24. He W, et al. Metastable energetic nanocomposites of MOF-activated aluminum featured with multi-level energy releases. Chem Eng J. 2020;381:122623.
25. Qu W, et al. Pb single atoms enable unprecedented catalytic behavior for the combustion of energetic materials. Adv Sci. 2021;8(5):2002889.
26. Wang R, et al. Preparation of quasi-core/shell structured composite energetic materials to improve combustion performance. RSC Adv. 2023;13(26):17834–41.
27. He W, et al. Energetic metastable n-Al@ PVDF/EMOF composite nanofibers with improved combustion performances. Chem Eng J. 2020;383:123146.
28. Lu Z, et al. In situ synthesis of silver nanoparticles uniformly distributed on polydopamine-coated silk fibers for antibacterial application. J Colloid Interface Sci. 2015;452:8–14.
29. Khawam A, Flanagan DR. Basics and applications of solid-state kinetics: a pharmaceutical perspective. J Pharm Sci. 2006;95(3):472–98.
30. Trache D, Abdelaziz A, Siouani B. A simple and linear isoconversional method to determine the pre-exponential factors and the mathematical reaction mechanism functions. J Therm Anal Calorim. 2017;128(1):335–48.
31. Muldowney P. A modern theory of random variation: with applications in stochastic calculus, financial mathematics, and Feynman integration. Hoboken: John Wiley & Sons; 2013.
32. Vyazovkin S, et al. ICTAC Kinetics Committee recommendations for performing kinetic computations on thermal analysis data. Thermochim Acta. 2011;520(1–2):1–19.

33. Trache D, et al. Physicochemical properties of microcrystalline nitrocellulose from Alfa grass fibres and its thermal stability. J Therm Anal Calorim. 2016;124(3):1485–96.
34. Gao Y, et al. Catalyzed combustion of a nanofluid fuel droplet containing polydopamine-coated metastable intermixed composite n-Al/CuO. Aerosp Sci Technol. 2021;118:107005.
35. Yadav N, Srivastava PK, Varma M. Recent advances in catalytic combustion of AP-based composite solid propellants. Def Technol. 2020.
36. Peng L, et al. Microwave-assisted deposition of silver nanoparticles on bamboo pulp fabric through dopamine functionalization. Appl Surf Sci. 2016;386:151–9.
37. Liao Y, et al. Antibacterial surfaces through dopamine functionalization and silver nanoparticle immobilization. Mater Chem Phys. 2010;121(3):534–40.
38. Du S, et al. New insights into the formation mechanism of gold nanoparticles using dopamine as a reducing agent. J Colloid Interface Sci. 2018;523:27–34.
39. Chen J, et al. Catalytic co-pyrolysis of 5-Amino-1H-Tetrazole assembled with copper and boron powder: pyrolysis kinetics and reaction mechanism. Fuel. 2022;314:122783.